ELSEVIER

Physica C 274 (1997) 1–8

PHYSICA C

Tunneling in anisotropic gap superconductors

J. Bok, J. Bouvier *

Laboratoire de Physique du Solide UPR 5 CNRS, ESPCI, 10 rue Vauquelin, 75231 Paris Cedex 05, France

Received 26 July 1996; revised manuscript received 22 October 1996

Abstract

We report a calculation of the density of states (DOS) of quasi-particle excitations in the superconducting state of high T_c cuprates using a model of the anisotropic gap that we have recently developed [1]. This model is based on the van Hove scenario, that is on the assumption that the Fermi level lies close to singularities in the DOS. We compare this theoretical DOS to the results obtained in various tunneling experiments especially with break junction [2,3] (S–I–S) and with vacuum scanning tunneling spectroscopy [4] (N–I–S). The agreement is very good. We explain the structure observed in the gap; and with the van Hove singularity slightly below the Fermi level we reproduce the observed asymmetry in the conductance and the dip in the DOS that is also seen in photoemission [5].

PACS: 74.20.-z; 74.20.Fg; 74.50.+r; 74.70.Vy

Keywords: Superconductivity; Anisotropic gap; Van Hove singularities; Tunneling spectroscopy

1. Introduction

Tunneling spectroscopy has been very important in verifying the BCS theory of conventional superconductors. The conductance of a normal–insulator–superconductor (N–I–S) junction is directly proportional to the quasi-particle density of states (QP DOS) and gives a precise and direct measurement of the superconducting gap. For a superconductor with an isotropic (s-wave) gap Δ_0, the BCS prediction for the QP DOS is

$$N_{\mathrm{BCS}}(\epsilon)=\begin{cases} N_0\dfrac{|\epsilon|}{\left(\epsilon^2-\Delta_0^2\right)^{1/2}} & \text{for } |\epsilon|>\Delta_0, \\ 0 & \text{for } |\epsilon|<\Delta_0, \end{cases}$$

where N_0 is the constant DOS in the normal state.

We extend the calculation of $N_S(\epsilon)$ to the case of a two-dimensional superconductor with a saddle point in the band structure and an anisotropic gap Δ_k of the form

$$\Delta_k=\Delta_0+\Delta_1\cos 4\Phi,$$

where Φ is given by $\tan\Phi=k_y/k_x$ such as the one calculated by the authors in a previous paper [1].

* Corresponding author. Fax: +33 1 40 79 44 25; e-mail: jacqueline.bouvier@espci.fr.

PII S0921-4534(96)00642-9

Various experiments have been performed to directly measure the gap and its anisotropy in HTCS. Let us only quote two approaches.

1. Angular resolved photoemission: three groups [5–7] have reported data on five high T_c compounds. In all these crystals, van Hove singularities have been observed close to the Fermi level. The best data have been obtained for BiSrCuCaCuO (2212) where a maximum gap between 20 and 30 meV, and a minimum gap between 0 and 10 meV are measured. The difficulty involved in these experiments is preparing a clean and well defined surface and the extreme precision required; millivolts are measured starting from 20 eV photons.

2. Tunneling spectroscopy. In the case of HTS, tunneling spectroscopy is still awaiting acceptance in the scientific community, as the experimental data are widely scattered. This is essentially due to the difficulty of preparing good tunnel junctions. These difficulties are the consequence of the very short coherence length in these materials and the high chemical reactivity of their surfaces. Nevertheless some convergent results have been reported recently [8]. The best results have been obtained in BiSrCaCuO (2212) with break junction [3] and vacuum tunnel spectroscopy [4], some results exist also for YBaCuO (123) [9–11]. The main results are a maximum gap between 19 and 30 meV, giving an average ratio $2\Delta/k_BT_c \approx 6$, a minimum gap between 0 and 12 meV, a normal density of states with a negative curvature (which is very different from classical superconductors), and a dip below the peak corresponding to the maximum gap (Δ_M) in some N–I–S junctions.

In this paper we propose a model which gives a direct interpretation of these results. We compute the density of states of a two-dimensional superconductor with a band structure given by

$$\xi_k = -2t(\cos k_x a + \cos k_y a) + \delta, \tag{1}$$

where ξ_k is the energy of itinerant electrons measured from the Fermi level. This structure presents saddle points for $\delta = 0$, $\xi_k = E_S$ and a van Hove singularity (vHs) in the normal density of states. We then apply this calculation to the $I(V)$ characteristic of N–I–S and S–I–S tunnel junctions and compare it to the experimental result.

2. Calculation of the quasi-particle excitations DOS

We use the itinerant electron model in a two-dimensional space that we have previously taken to compute an anisotropic gap using the BCS gap equation. The band structure is given by Eq. (1). We shall first perform the calculation in the case $\delta = 0$, i.e. where the vHs coincides with the Fermi level E_F. The following form for the gap is obtained:

$$\Delta_k = \Delta_0 + \Delta_1 \cos 4\Phi, \tag{2}$$

where Δ_0 is the average gap which obeys the relation $2\Delta_0/k_BT_c = 3.7$.

The maximum gap is $\Delta_M = \Delta_0 + \Delta_1$ in the direction of the saddle points $(0, \pm\pi)$ and $(\pm\pi, 0)$ and the minimum gap is $\Delta_m = \Delta_0 - \Delta_1$ at $\Phi = \pi/4$. By fitting with values from photoemission experiments, we found $2\Delta_M/k_BT_c \approx 6$ and $2\Delta_m/k_BT_c \approx 2$. These values are close to those observed in tunneling experiments.

Remaining in a weak coupling model with λ_{eff} of the order of 0.4, we take a simplified version of Eq. (2) which makes the calculation easier:

$$\Delta_k = \Delta_M - \Delta_2 \sin^2 k_x a, \tag{3}$$

so that $\Delta_m = \Delta_M - \Delta_2$ is the minimum gap.

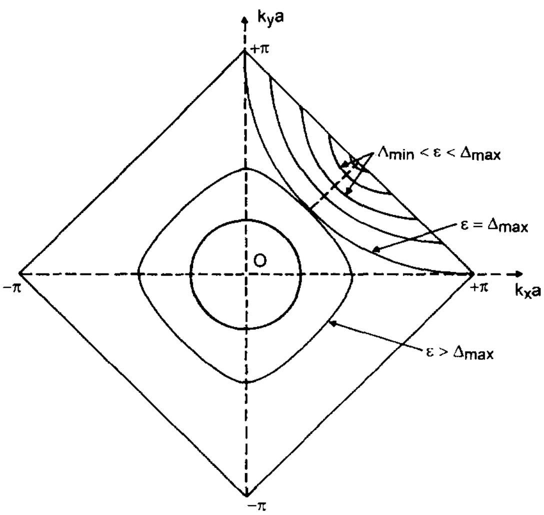

Fig. 1. Fermi surface and curves of constant energy ϵ_k. For clarity, the scale between Δ_M and Δ_m is expanded.

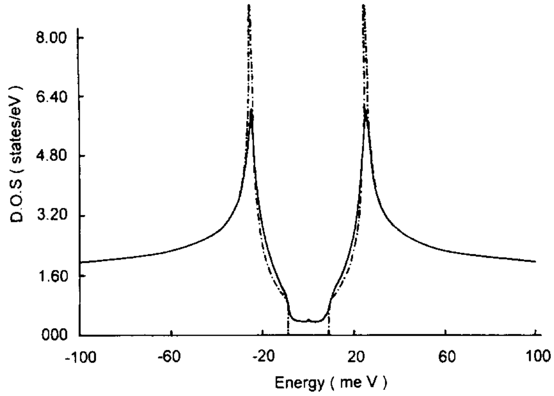

Fig. 2. DOS or conductance dI/dV at $T=0$ K calculated for a N–I–S tunneling junction. $\Delta_M = 25$ meV, $\Delta_m = 9$ meV, $t = 0.2$ eV. Dotted-dashed line: $\Gamma = 0$ meV, solid line: $\Gamma = 0.5$ meV.

Hence using the BCS theory we find for the energies ϵ_k of the excited states:

$$\epsilon_k^2 = \xi_k^2 + \Delta_k^2, \tag{4}$$

with $\xi_k = -2t(\cos k_x a + \cos k_y a)$, $\delta = 0$. The bandwidth in this case is $W = 8t$, photoemission experiments [5] have determined a value of t between 0.18 and 0.25 eV.

To compute the quasi-particle DOS ($N_S(\epsilon)$) in the superconducting state, we must first calculate the area $A(\epsilon)$ embraced by the curve of constant energy (Fig. 1), $\epsilon_k = \text{cte} = \epsilon$ given by Eq. (4) in k space (k_x, k_y plane), taking into account the spin degeneracy, then N_S is given by:

$$N_S(\epsilon) = \frac{1}{2\pi^2}\frac{\partial A}{\partial \epsilon}. \tag{5}$$

We have also taken into account a possible finite lifetime of the quasi-particle states, by introducing a phenomenological broadening Γ. We replace ϵ_k by $\epsilon_k - \mathrm{i}\Gamma$ in Eq. (4) and take the real part of $N_S(\epsilon)$.

The result of our calculation is given in Fig. 2 for $\Gamma = 0$ and $\Gamma = 0.5$ meV, and $\Delta_M = 25$ meV, $\Delta_m = 9$ meV, $t = 0.2$ eV. We see that the DOS is no longer zero for $\Delta < \Delta_M$, it starts at Δ_m with a step for $\Gamma = 0$, and with a shoulder for a finite Γ.

3. $I(V)$ characteristic of a tunnel junction

Since the first experiments by Giaever [12], many theoretical calculations of the $I(V)$ characteristic have been made. We follow the analysis given in the book by Wolff [13].

The general expression of the current in a tunnel junction is given by:

$$I(V) = C\int_{-\infty}^{+\infty} N_L(\epsilon) N_R(\epsilon + V)[f(\epsilon) - f(\epsilon + V)]\,\mathrm{d}\epsilon,$$

where C is a constant (independent of energy ϵ) proportional to $|T|^2$, the square of the transmission of the barrier; N_L and N_R are the DOS of the left and right electrodes respectively.

3.1. N–I–S tunnel junction

In this case the left electrode may be taken as normal so we may put $N_L = N_0 = \text{cte}$, and that the right one is the DOS of the superconductor so $N_R = N_S(\epsilon)$, following the formulae found in the book of Wolff [13], we have:

$$I(V) = CN_0\int_{-\infty}^{+\infty} N_S(\epsilon)[f(\epsilon) - f(\epsilon - V)]\,\mathrm{d}\epsilon$$

and

$$\frac{\mathrm{d}I}{\mathrm{d}V} = CN_0\int_{-\infty}^{+\infty} N_S(\epsilon)\left[-\frac{\partial f}{\partial \epsilon}(\epsilon - V)\right]\mathrm{d}\epsilon, \tag{6}$$

and at low temperature $k_B T \ll \Delta_m$, we have:

$$\mathrm{d}I/\mathrm{d}V = CN_0 N_S(V). \tag{7}$$

To compare with experiments, especially with vac-

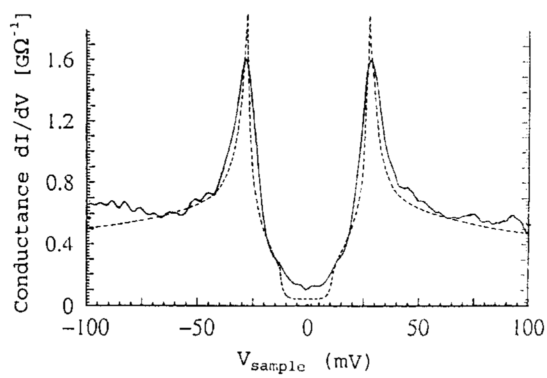

Fig. 3. The best fit of the conductance measured by tunneling spectroscopy on BSCCO, N–I–S junction, by Renner and Fischer (Fig. 10 of Ref. [4]). Dashed line is fitted curve with $\Delta_M = 27$ meV, $\Delta_m = 11$ meV, $t = 0.18$ eV, $\Gamma = 0.5$ meV at $T = 5$ K. Solid line is experimental curve.

uum tunnel spectroscopy [4,14], we shall use Eq. (6) at different temperatures.

The best results have been obtained on BSCCO (2212) by Renner and Fisher [4]. The best fit with their results (Fig. 10 of Ref. [4]) is obtained with the following set of parameters:

$\Delta_M = 27\,\text{meV}$, $\Delta_m = 11\,\text{meV}$, $t = 0.18\,\text{eV}$,

$\Gamma = 0.5\,\text{meV}$, $T = 5\,\text{K}$.

As the prefactor C is unknown we adjust the theoretical curve to the experimental one for $V \to \infty$. The results are given in Fig. 3. The agreement is very good. In particular if the shoulder seen at 12 meV is not an experimental artefact, it gives a direct measurement of the minimum gap.

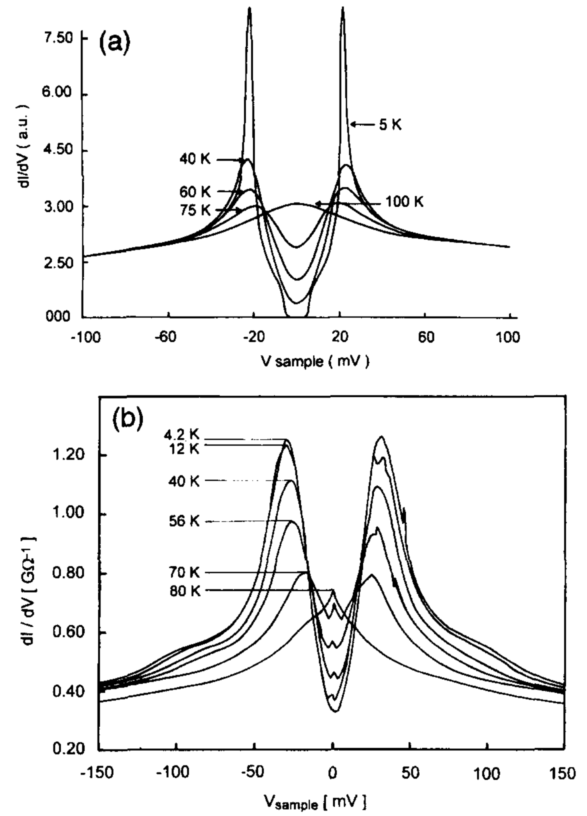

Fig. 4. (a) The temperature dependence of the conductance measured on a N–I–S junction. The set of the temperature dependence of the gaps come from our previous calculations (Ref. [1]). (b) Experimental curves of the tunnel characteristics of the N–I–S junction (Fig. 4 of Ref. [15]). Set of parameters (from Ref. [1]): $T = 5$ K $\Delta_M = 22$ meV, $\Delta_m = 6$ meV; $T = 40$ K $\Delta_M = 21.4$ meV, $\Delta_m = 5.8$ meV; $T = 60$ K $\Delta_M = 18.6$ meV, $\Delta_m = 5.1$ meV; $T = 75$ K $\Delta_M = 8.7$ meV, $\Delta_m = 3.7$ meV; $T = 100$ K $\Delta_M = \Delta_m = 0$ meV.

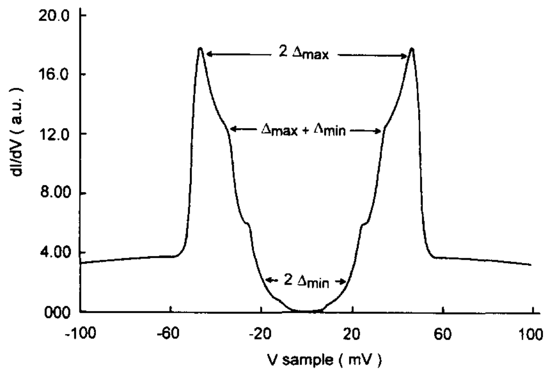

Fig. 5. Conductance of a S–I–S junction at $T = 0$ K, with $\Delta_M = 25$ meV, $\Delta_m = 9$ meV, $\Gamma = 0.5$ meV and $t = 0.2$ eV. The arrows show the main structures following from the superconducting DOS convolution.

We present in Fig. 4 the curves of the N–I–S junctions characteristics versus the temperature. We use our temperature dependence of the gaps previously calculated [1]. We can see that the behavior is similar to that observed by Tulina et al. [15] (Fig. 4 of Ref. [15]). The gap fills up under Δ_m.

3.2. S–I–S junctions

To interpret the results obtained with break junctions [2,3], we compute the $I(V)$ characteristic of a S–I–S junction, where S is an anisotropic gap superconductor.

At low temperature $I(V)$ is given by the convolution integral

$$I(V) = C\int_0^V N_S(\epsilon) N_S(\epsilon - V)\,\mathrm{d}\epsilon.$$

We compute this integral and then $\mathrm{d}I/\mathrm{d}V$ numerically. The results are given in Fig. 5 at $T = 0$ K. This curve shows some particular structures due to the convolution of the two DOS of the superconducting electrodes. The result is symmetric about zero voltage.

4. The van Hove singularity is not exactly at E_F

Finally we examine the case where the saddle point is not at the same energy E_S as the Fermi level

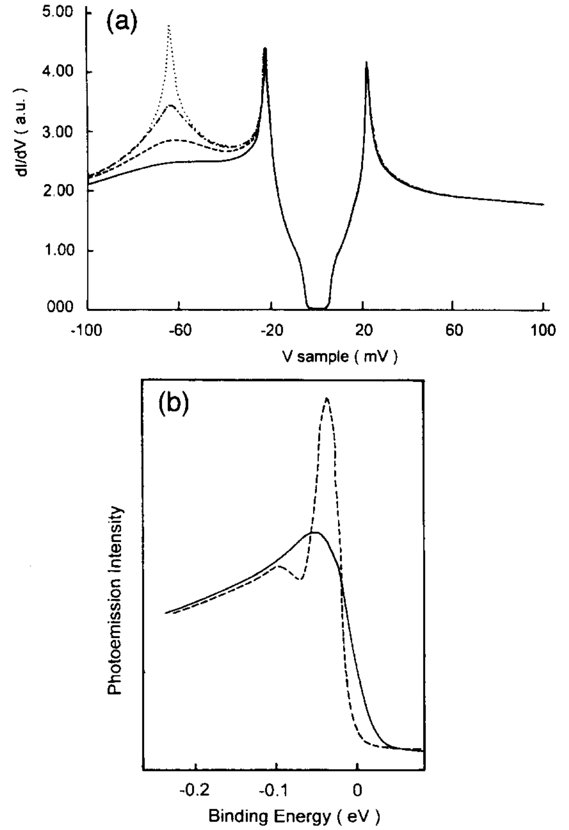

Fig. 6. (a) Curves of the conductances calculated for a N–I–S junction, with the position of E_S $\delta = -60$ meV, and different values of the empirical lifetime Γ' at the logarithmic singularity E_S. At $T = 5$ K, with $\Delta_M = 22$ meV, $\Delta_m = 6$ meV, $\Gamma = 0.1$ meV and $t = 0.2$ eV. Dotted line: $\Gamma' = 0$ meV, dotted-dashed line: $\Gamma' = 5$ meV, dashed line: $\Gamma' = 15$ meV, solid line: $\Gamma' = 30$ meV. (b) Photoemission measurement from Hwu et al. (Ref. [16]). Solid line: normal state, dashed line: superconducting state.

E_F. The position E_S of the van Hove singularity depends only on the band structure of the crystal whereas E_F is dependent on the density of holes, that is on the doping. Hence for a given compound such as YBaCuO(123) or BiSrCaCuO(2212), the distance $E_F - E_S$ varies with doping between different samples.

We take $E_F = 0$, so that the band structure is given by

$$\xi_k = -2t(\cos k_x a + \cos k_y a) + \delta, \tag{8}$$

with $\delta = E_S - E_F$

We take $\delta < 0$, i.e. E_S below the Fermi level and for the quasi-particles excitations, we still have formula (4)

$$\epsilon_k^2 = \xi_k^2 + \Delta_k^2.$$

We compute the DOS using the same procedure as before; we compute numerically the area $A(\epsilon)$ embraced by a constant energy curve ($\epsilon = \text{cte}$) and we take

$$N(\epsilon) = \frac{1}{2\pi^2}\frac{\partial A}{\partial \epsilon}.$$

The result of the corresponding conductance is given in Fig. 6. We see that we have now three

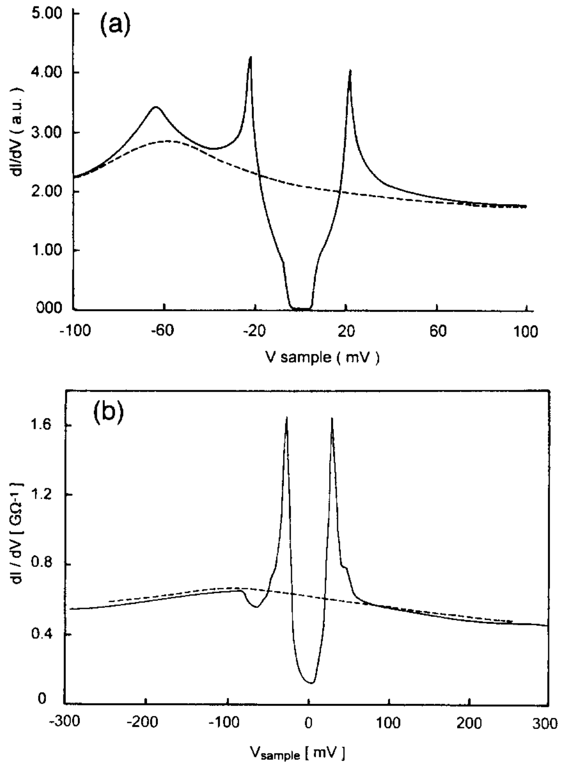

Fig. 7. (a) Curves of the conductance calculated for a N–I–S junction. Solid line: in the superconducting state at $T = 5$ K with $\Delta_M = 22$ meV, $\Delta_m = 6$ meV, $\Gamma = 0.1$ meV, $t = 0.2$ eV and $\delta = -60$ meV, $\Gamma' = 5$ meV. Dashed line: in the normal state at $T = 100$ K with $\Delta_M = \Delta_m = 0$ meV, $\Gamma = 0.1$ meV, $t = 0.2$ eV and $\delta = -60$ meV, $\Gamma' = 5$ meV. (b) For comparison we show Fig. 7 of Ref. [4]. The maximum of the normal state conductance (or DOS) at negative sample bias is well reproduced.

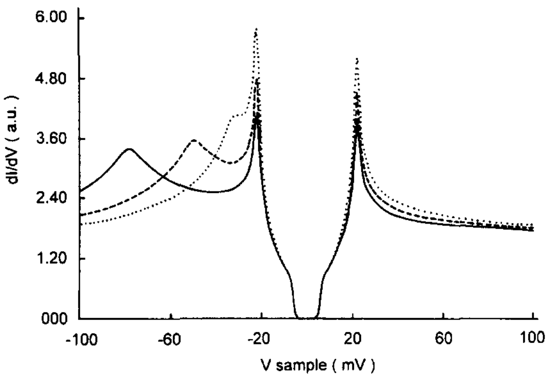

Fig. 8. Curves of the conductances calculated for a N–I–S junction, with different values of the position δ of E_S. At $T = 5$ K, with $\Delta_M = 22$ meV, $\Delta_m = 6$ meV, $\Gamma = 0.1$ meV and $t = 0.2$ eV. Solid line $\delta = -75$ meV, dashed line $\delta = -45$ meV, dotted line $\delta = -25$ meV.

singularities, two at $\pm \Delta_M$ as for a classical superconductor, and a third one at a negative energy $-E_1$. Between $-E_1$ and $-\Delta_M$ we find a dip which has been observed both in photoemission [16] and in tunneling spectroscopy [4]. The two singularities at $\pm\Delta_M$ are square root singularities, the DOS varies as $(\epsilon^2 - \Delta_M^2)^{-1/2}$, the singularity at $-E_1$ is logarithmic like a 2D vHs. We can easily find that result using a simplified model. Let us take an isotropic gap $\Delta_k = \text{constant} = \Delta$ and ξ_k still given by Eq. (8). We get

$$N_S(\epsilon) = \frac{1}{2\pi^2} \frac{\partial A(u)}{\partial u} \frac{\partial u}{\partial \epsilon},$$

where $u = \pm\sqrt{\epsilon^2 - \Delta^2}$, but $[1/(2\pi^2)][\partial A(u)/(\partial u)]$ is nothing else than $N_N(u)$, the DOS in the normal state so that

$$N_S(\epsilon) = N_N(u) \frac{|\epsilon|}{\sqrt{\epsilon^2 - \Delta^2}}. \tag{9}$$

However we know that in the normal state the saddle point in 2D gives a logarithmic singularity

$$N_N(u) = -N_0 \ln \frac{|u - E_S|}{D},$$

where D is the width of the vHs, so that

$$N_S(\epsilon) = -N_0 \left[\ln \frac{\left|\sqrt{\epsilon^2 - \Delta^2} + E_S\right|}{D} \right] \frac{|\epsilon|}{\sqrt{\epsilon^2 - \Delta^2}} \tag{10}$$

for $\epsilon < 0$ and $E_S < 0$, and

$$N_S(\epsilon) = -N_0 \left[\ln \frac{\left|\sqrt{\epsilon^2 - \Delta^2} - E_S\right|}{D} \right] \frac{\epsilon}{\sqrt{\epsilon^2 - \Delta^2}}$$

for $\epsilon > 0$ and $E_S < 0$.

We see clearly the three singularities with

$$E_1^2 = E_S^2 + \Delta^2. \tag{11}$$

Formula (11) is a good approximation for the actual case (Δ_k anisotropic) that we have computed numerically and which is represented in Fig. 6.

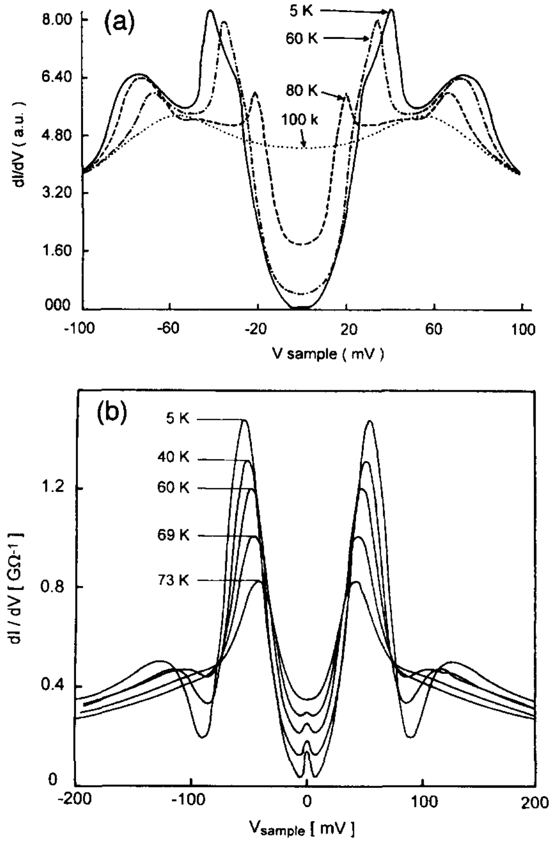

Fig. 9. (a) Curves of the temperature dependence of the conductance calculated for a S–I–S junction with the set of gaps(T) calculated in Ref. [1]. Solid line: $T = 5$ K $\Delta_M = 22$ meV, $\Delta_m = 6$ meV, dashed line: $T = 60$ K $\Delta_M = 18.6$ meV, $\Delta_m = 5.1$ meV, dotted-dashed line: $T = 80$ K $\Delta_M = 10.8$ meV, $\Delta_m = 2.95$ meV, dotted line: $T = 100$ K $\Delta_M = \Delta_m = 0$ meV. (b) Experimental curves of Mandrus et al. (from Ref. [2]).

In the actual samples, we have various impurities and crystalline defects (disorder), so that the singularities are damped. To take into account these effects, we introduce two empirical lifetimes Γ and Γ'.

Γ is a pair breaking lifetime and is characteristic of the superconducting state. It gives a broadening of the peaks at $\pm\Delta_M$, we have seen before that Γ is of the order of 0.5 meV.

Γ' takes into account the effects which broaden or even destroy the logarithmic singularity. This vHs is very sensitive to disorder in the CuO_2 planes (the v.H. theorem is only valid for a periodic potential) and to a coupling in the third dimension.

Γ' is of the order of 5 to 30 meV by comparison of our theory with the experimental results. This comparison is given in Figs. 6 and 7. The position of E_S can move versus the doping, this is represented Fig. 8.

In Fig. 9 we plot the temperature dependence of the S–I–S junctions characteristics. The symmetric dip disappears when the temperature increases, this is observed in the experimental curves of Mandrus et al. (Fig. 1 of Ref. [2]).

5. Conclusion

We see that this model is in excellent agreement with a great number of experimental results. The main features that it predicts in tunneling spectroscopy are:

1. Structures are seen in the gap between the maximum gap Δ_M and the minimum gap Δ_m.

2. The normal density of states has a maximum at an energy close to E_F. The curvature is downwards and not constant, or upwards, like in classical superconductors.

3. A dip is seen in the DOS on the left side only of the gap (asymmetry of the $I(V)$ characteristic). This dip is also seen in photoemission experiments [16] and is well explained, assuming that $E_S < E_F$.

4. The dip moves towards the right for overdoped samples, this is in concordance with the fact that the distance $E_F - E_S$ is getting smaller with increasing doping. That is experimentally observed [17].

5. The predicted variation of the dI/dV curve with temperature is observed experimentally.

6. The sum rule is verified. The total number of states is conserved between the normal and superconducting state.

A detailed adjustment between our calculations and the experimental results is not always possible. It is very precise and quantitative in Fig. 3 with the result of Renner et al. [4] and more qualitative in other cases. But the important features are always present.

This discrepancy can be due to several reasons. Some are theoretical, our model is simplified, we do not take into account the antiferromagnetic fluctua-

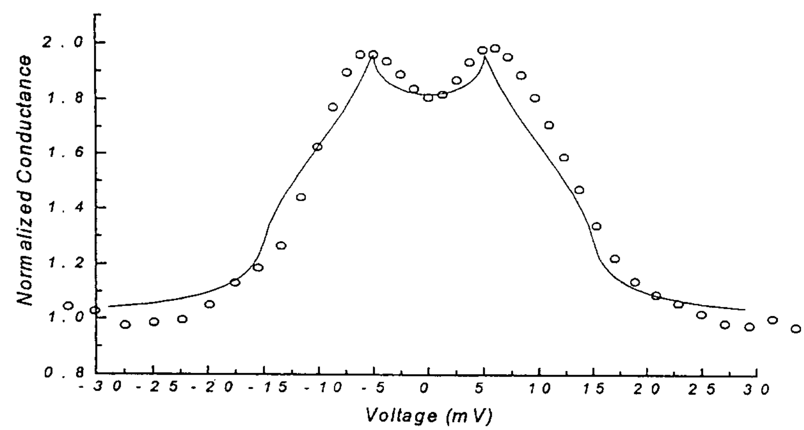

Fig. 10. Andreev reflection results of Achsaf et al. [18]. Open circles: experimental results, line: extended s-wave fit, with $\Delta_M = 15$ meV, $\Delta_m = 5$ meV.

tions nor the phonon contribution to dI/dV. Others are experimental, in all papers, the authors point out the great difficulty to make "clean" experiments. They meet many problems: the quality of the sample surface, its high chemical reactivity [15], the quality of the insulating barriers, the problem of the current distribution in the surface [3], the experimental resolution of the various peaks and shoulder [4], the temperature calibration, the heating effects [2], etc.

Nevertheless we think that our itinerant electron model, with a normal band structure showing four saddle points (van Hove singularities), and with an anisotropic gap varying from Δ_M in the directions of the vHs to Δ_m at an angle of $\pi/4$, gives a very good description of all phenomena observed in tunnel spectroscopy and angular resolved photoemission.

6. Note added in proof

Recently Achsaf et al. [18] have measured Andreev reflections at an interface between a gold tip and a $La_{2-x}Sr_xCuO_4$ single crystal along the 110 direction. The best fit of their data is obtained for an anisotropic gap (our formula (2)) with $\Delta_M = 15$ meV and $\Delta_m = 5$ meV. The variation of the conductance with applied voltage shows clearly two peaks corresponding to $\pm\Delta_m$ (Fig. 10).

Acknowledgements

This work has been supported by D.R.E.T., under contract # 94-070.

References

[1] J. Bouvier and J. Bok, Physica C 249 (1995) 117.
[2] D. Mandrus, J. Hartge, C. Kendziora, L. Mihaly and L. Forro, Europhys. Lett. 3 (1993) 199.
[3] S.I. Vedeneev, A.G.M. Jansen, P. Samuely, V.A. Stepanov, A.A. Tsvetkov and P. Wyder, Phys. Rev. B 49 (1994) 9823.
[4] Ch. Renner and Ø. Fischer, Phys. Rev. B 51 (1995) 9208.
[5] Z.X Shen, W.E. Spicer, D.M. King, D.S. Dessau and B.O. Wells, Science 267 (1995) 343.
[6] H. Ding, J.C. Campuzano, K. Gofron, C. Gu, R. Liu, B.W. Veal and J. Jennings, Phys. Rev. B 50 (1994) 1333.
[7] J. Ma, C. Quitmann, R.J. Kelley, P. Almeras, H. Berger, G. Margaritondo and M. Onellion, Phys. Rev. B 51 (1995) 3832.
[8] T. Hasegawa, H. Ikuta and K. Kitazawa, in: Physical Properties of High Temperature Superconductors III, ed. D.M. Ginzberg (World Scientific, Singapore, 1992).
[9] Ya.G. Ponomarev, N.B. Brandt, Chong Soon Khi, S.V. Tchesnokov, E.B. Tsoku, A.V. Yarigin, K.T. Yusupov, B.A. Aminov, M.A. Herin, G. Müller, H. Piel, D. Wehler, V.Z. Kresin, K. Rosner, K. Winzer and Th. Wolf, Phys. Rev. B 52 (1995) 1352.
[10] E. Polturak, G. Koren, D. Cohen and E. Aharoni, Phys. Rev. B 47 (1993) 5270.
[11] Nin Haas, D. Ilzycer, G. Deutscher, G. Desgardin, I. Monot and M. Weger, J. Supercond. 5 (1992) 191.
[12] I. Giaever, Phys. Rev. Lett. 5 (1960) 147; 5 (1960) 464.
[13] E.L. Wolf, Principles of Electron Tunneling Spectroscopy (Oxford University Press, Oxford, 1989).
[14] I. Maggio-Aprile, Ch. Renner, A. Erb, E. Walker and Ø. Fischer, Phys. Rev. Lett. 75 (1995) 2754.
[15] N.A. Tulina, S.V. Zaitsev, G.A. Emel'chenco and A.B. Kulakov, Physica C 248 (1995) 359.
[16] Y. Hwu, L. Lozzi, M. Marsi, S. La Rosa, M. Winuku, P. Davis, M. Onellion, H. Berger, F. Gozzo, F. Levy and G. Margaritondo, Phys. Rev. Lett. 67 (1991) 2573.
[17] Ch. Renner and Ø. Fischer, private communication.
[18] N.S. Achsaf, D. Goldschmidt, G. Deutscher, A. Revcolevschi and A. Vietkine, preprint, to be published in Proc. M.O.S., Karlsruhe, August 1996 (J. Supercond.).